Modeling and Understanding Closed-Loop Liquid−Liquid Immiscibility in Aqueous Solutions of Poly(ethylene glycol) Using the SAFT-VR Approach with Transferable Parameters

Gary N. I. Clark,[†] Amparo Galindo,*[,†] George Jackson,[†] Steve Rogers,[‡] and Andrew N. Burgess[‡]

Department of Chemical Engineering, Imperial College London, South Kensington Campus, London SW7 2AZ, U.K., and ICI Strategic Technology Group, Wilton Centre, PO Box 90, Redcar TS90 8JE, U.K.

Received April 9, 2008; Revised Manuscript Received June 16, 2008

ABSTRACT: The closed-loop liquid−liquid fluid phase equilibria of aqueous solutions of poly(ethylene glycol) (PEG) binary mixtures are studied using the statistical associating fluid theory for potentials of variable range (SAFT-VR). A molecular model of the mixture is developed which takes into account the delicate balance between the water−water, water−PEG, and PEG−PEG hydrogen-bonding interactions as well as the usual repulsive and attractive/dispersive contributions. A fully transferable intermolecular potential model is proposed which allows one to study any aqueous PEG system with the molecular weight of the polymer as sole input. An excellent predictive description of the liquid−liquid phase behavior of these systems is achieved; mixtures involving shorter polymers are used to determine the binary (unlike) interaction parameters, and we are then able to predict the phase behavior of mixtures of larger molecular weight in good agreement with experimental data. The high-pressure (GPa) phase behavior of the liquid−liquid phase equilibria in these systems is also studied. The region of closed-loop immiscibility is seen to become less extensive with an initial increase in pressure. For intermediate molecular weights (2000 $\lesssim$ MW $\lesssim$ 100 000 g/mol) of the polymer the liquid phase becomes homogeneous when the pressure is increased beyond a high enough threshold, and at even higher pressures a second region of liquid−liquid separation is observed. In the case of high molecular weight polymers (MW $\gtrsim$ 100 000 g/mol) the fluid phase behavior is characterized by an hourglass-shaped region of immiscibility with liquid−liquid separation persisting for all pressures considered. The dome-shaped regions of liquid−liquid immiscibility predicted for aqueous solutions of PEG of intermediate molecular weight (2000 $\lesssim$ MW $\lesssim$ 75 000 g/mol) are reminiscent of the pressure−temperature denaturation boundaries found in protein systems which are thought to be governed by a corresponding increase in water solubility into the hydrophobic core.

1. Introduction

Poly(ethylene glycol), PEG (H−[O−CH_2−CH_2]$_n$−OH), is composed of a number n of ethylene oxide repeat units, terminated at both ends with a hydroxyl group. The molecules of high molecular weight are also commonly denoted as "poly(ethylene oxide) (PEO)" to refer to polymers that are methyl-terminated at either or both ends of the molecule. In this work we consider the hydroxyl-terminated molecules, denoting them as PEG, but when referring to the work of other authors we employ their terminology.

Formulations incorporating PEG are widely used in industry due to the solubility of the polymer in water and in many organic solvents, finding applications in paints, detergents, soap, paper making, defoamers, lubricants, softeners, and adhesives, to name but a few. Because of its ability to resist cell and protein adhesion and recognition by the immune system, it is also a widely used and accepted biomaterial.[1] There is a large body of work on the structure, function, and application of PEG. In our study we are interested in its fluid phase behavior in aqueous solution, where closed loops of liquid−liquid immiscibility can be observed. The effect of pressure and polymer molecular weight on this closed-loop liquid−liquid immiscibility is of particular interest, as is the underlying thermodynamic behavior that triggers the immiscibility.

One of the first to investigate the phase behavior of PEG in aqueous solution were Malcolm and Rowlinson,[2] who observed that the homogeneous liquid phase separates into two coexisting liquid phases as the temperature was lowered below an upper critical solution temperature (UCST). On further lowering of the temperature below the lower critical solution temperature (LCST) the mixture becomes homogeneous once again, resulting in a closed-loop region of liquid−liquid immiscibility. This type of phase equilibria was first reported in mixtures of water + nicotine,[3] and a variety of systems are now known to exhibit this behavior (see the review in ref 4). Malcolm and Rowlinson examined the phase diagram of aqueous solutions of PEG-3000 and PEG-5000 and noted the molecular-weight dependence of the closed-loop region of immiscibility. Note that we use the terminology "PEG-MW" to denote the number-average molecular weight (MW in g/mol) of the polymer in question, e.g., "PEG-2180". The closed loops are seen to shrink as the molecular weight is decreased, and the limit of immiscibility is found for PEG-2140, which is completely soluble in water.[5] The effect of pressure is also of interest. An increase in pressure can lead to increased miscibility and hence smaller closed loops; at high-enough pressure a double critical end point is found where the LCST and UCST meet and the loop disappears. This behavior has been reported for example for the mixture water + butoxyethanol.[6−8] The pressure dependence of the LCST in PEG solutions was studied by Saeki et al.,[5] who find little change in the LCST values for a solution of PEG-1 020 000 in the range of pressures below 5 MPa. Recent reports suggest an increase in immiscibility, with a dramatic lowering of the LCST at pressures of ∼450 MPa. This phenomenon was first reported by Cook et al.[9] for a mixture of water + PEG-270 000. Sun and King[10] subsequently reported the same type of behavior for mixtures with PEG-21 000 and PEG-1 390 000 and also noted the existence of a maximum in pressure which leads to

* Corresponding author. E-mail: a.galindo@imperial.ac.uk.
[†] Imperial College London.
[‡] ICI Strategic Technology Group, Wilton Centre.

10.1021/ma8007898 CCC: $40.75
Published on Web 08/09/2008

re-entrant behavior manifesting itself as an additional region of "miscibility" in the system at very low temperatures. The increased immiscibility seen at high pressures has been explained in terms of the disruption of hydrogen bonds with significant compression of the system. Briscoe et al.[11] have studied the effect of pressure, added salts, and diluents, reaching similar conclusions, and more recently Hammouda et al.[12] have confirmed this view from an analysis of the data of small-angle neutron scattering experiments. All polymers are to some extent polydisperse, and it is known that polydispersity can have a considerable effect on the detailed phase behavior of polymer solutions. PEG can be obtained, however, as reasonably monodisperse samples. Sun and King[10] mention polydispersity indices for their experiments of 1.17 and 1.15, and Saeki et al.[5] use the solution fractionation technique to reduce the polydispersity of their samples. For consistency, in this work we have interpreted the experimental data always as number-average molecular weights.

The UCST associated with liquid−liquid separation is understood to be a consequence of the positive entropic contribution due to mixing ($\Delta S_m > 0$), which becomes more important with increasing temperature overcoming the unfavorable enthalpy of mixing ($\Delta H_m > 0$), which is the underlying cause of the immiscibility. Though the thermodynamic driver behind the UCST in fluid systems is always of the same energetic nature, this is not the case for the LCST. Two very different thermodynamic mechanisms are behind the onset of immiscibility at an LCST: one is a consequence of an increase in hydrogen bonding (or another type of specific attractive interaction) with decreasing temperature and can thus be classified as an enthalpy-driven transition ($\Delta H_m > 0$);[4,13] the other is caused by the size asymmetry between components, usually explained in terms of a contraction of the volume on mixing ($\Delta V_m < 0$), also referred to as a compressibility effect, and the dominant contribution that it can have on the entropy of mixing ($\Delta S_m < 0$).[13,14] Associated with these two very different mechanisms, two types of LCST behavior can be ascribed to the fluid phase equilibria exhibited by polymer solutions: a "high"-temperature LCST, invariably in a region close to the vapor−liquid critical point of the solvent (e.g., for solutions of polyethylene in *n*-pentane[15]), and a "low"-temperature LCST that appears well within the liquid region, below a UCST (as is found for aqueous solutions of PEG[2,5]). A good example of "low"-temperature LCST phase behavior which is thought to be driven by hydrogen bonding is exhibited in aqueous solutions of alkyl polyoxyethylene surfactants $H-[CH_2]_n-[O-CH_2-CH_2]_m-OH$ (see ref 16 and references therein). When the temperature is decreased, the extent of hydrogen bonding between unlike species gives rise to a favorable change in enthalpy $\Delta H_m < 0$, resulting in a transition from a demixed state to a homogeneous state. It has been suggested that the "low"-temperature LCST seen in the phase behavior of aqueous mixtures of PEG is also a result of hydrogen bonding.[17−19] In the context of this discussion it is also useful to mention the recent work of Ryu et al.,[20] who have reported closed-loop behavior for a blend of polystyrene + poly(*n* -pentyl methacrylate). The LCST of this system is explained by the authors as driven by compressibility (entropic) effects. On first inspection one may associate this type of behavior with the closed-loop immiscibility seen in aqueous mixtures well inside the liquid region of the phase diagram (which as explained earlier is driven by enthalpic contributions). However, the temperature range in polymer blends takes on a different meaning due to the sensitivity of the fluid phase behavior to the specific intermolecular interactions, and a certain degree of caution is advisible in making comparisons with the behavior seen in blends with that in mixtures of low molecular weight compounds or polymer solutions.

Hirschfelder et al.[21] were the first to postulate that the phase behavior of systems with an LCST was due to short-range orientational forces such as those responsible for hydrogen bonding. One of the earliest models developed to investigate this was the lattice model of Barker and Fock,[22] who used orientation-dependent contact points on molecules in a two-component mixture together with a quasi-chemical (mean-field) approach to obtain a closed-loop coexistence curve exhibiting both an LCST and a UCST. Wheeler[23] later developed a similar, simpler, model that could be mapped onto a spin-$^1/_2$ Ising lattice and solved without the need for a mean-field approximation. He obtained broader (in composition) regions of closed-loop immiscibility that were in better agreement with experimental data and which had the correct critical exponents. Only small "spherical" molecules were examined within these lattice models. The first molecular approach to treat the thermodynamic properties and fluid phase equilibria of polymer systems is attributed to Flory[24] and to Huggins.[25] By describing the polymers as chain molecules distributed on lattice sites with the remaining sites occupied by the solvent, expressions for the entropy and enthalpy of mixing as a function of the compositions and volume fractions of the components can be developed. An identical expression for the entropy of mixing to that of Flory and Huggins was also derived by Staverman and van Santen[26] in the same year. To date, the largest body of work in the description of the fluid phase behavior of aqueous solutions of PEG mixtures involves the use of approaches which are based on the lattice theory of Flory and Huggins, extended to account for hydrogen-bonding interactions.

By incorporating directional interactions into lattice models, one can capture the LCST of aqueous solutions of PEG. Karlström[27] has included such interactions in a Flory−Huggins approach by using two kinds of polymer segment (hydrophilic and hydrophobic) based on a conformational argument of a trans−gauche equilibrium between the C−O bonds and C−C bonds within the polymer chain. This equilibrium can be thought to lead to "segments" with an overall dipole moment (hydrophilic) and "segments" without (hydrophobic) that Karlström called "low"- and "high"-temperature states, respectively. Through the use of four χ enthalpic mixing parameters and a relation for the relative proportion of the two types of temperature state, Karlström obtained a semiquantitative description of the phase behavior of water + PEG mixtures of various molecular weights. In another study Hu et al.[28] have used a decorated-lattice model, based on a Flory−Huggins lattice where the underlying polymer solution is described by a fully occupied primary lattice, and a secondary Ising lattice is introduced as a perturbation to account for directional interactions. A good description was obtained for $T-x$ coexistence curves of water + PEG-3000 and water + PEG-5000. Hydrogen bonding in water−PEO systems has also been accounted for by Matsuyama and Tanaka,[29] who proposed a model to study the possible mechanisms for the appearance of LCSTs by examining the extent of hydration of PEO as a function of temperature. They concluded that hydrogen bonding between the water molecules and the ether oxygens of PEO is responsible for the LCST and the corresponding closed-loop region of liquid−liquid immiscibility due to a rapid decrease in the water solvation of the polymer as the temperature is increased in the neighborhood of the LCST. In interesting recent studies of water + PEO mixtures, Dormidontova[30,31] has accounted for the competition between different types of hydrogen bond by introducing water−water[30] and then PEO−PEO (i.e., hydroxyl-terminated PEO, or PEG using our terminology)[31] hydrogen bonding using a mean-field model. Dormidontova concluded that the inclusion

of water−water hydrogen bonding is of crucial importance in order to provide the correct description of the fluid phase behavior of water + PEO. The hydroxyl-terminated PEO was also found to be considerably more soluble than the methyl-terminated PEO for low molecular weights, in agreement with experimental expectations.

Using a lattice-type group contribution approach based on UNIFAC (which in turn employs a quasi-chemical treatment), Tritopoulou et al.[17] have also modeled the water + PEG system. Hydrogen bonding is not modeled explicitly; instead, aqueous solutions of PEG are treated as mixtures of two PEG groups (the terminal hydroxyl group and the ethylene oxide repeat unit) and the water molecule group. The model requires a knowledge of the molar volumes of water and PEG, the van der Waals volumes and surface areas of the three groups, and the temperature-dependent pair unlike binary interaction parameters. The interaction parameters are obtained by correlating activity coefficient data for a number of appropriate binary mixtures, apart for the interaction between the bulk ethylene oxide groups and water which is characterized by using experimental liquid−liquid equilibrium (LLE) data for a water + PEG-2190 mixture. Tritopoulou et al. obtained a good description of the closed-loop liquid−liquid immiscibility for a range of PEG molecular weights. The excess mixing functions for a range of temperatures are also examined in the case of water + PEG-2190. They found that a favorable enthalpy of mixing ($\Delta H_m < 0$) governs the low-temperature homogeneous behavior; with increasing temperature and the onset of an LCST, the unlike interactions become weaker and unfavorable dispersion interactions dominate. Interestingly, Tritopoulou et al. could not obtain a qualitative description when the terminal hydroxyl groups are not incorporated in the treatment, highlighting their importance for low molecular weight PEG polymers.

All of the theoretical approaches discussed thus far correspond to fully occupied lattice models, and as a consequence compressibility effects are neglected. The dependence on the pressure can be accounted for by introducing vacancies in the Flory−Huggins lattice description, as for example in the lattice−fluid theories of Sanchez and Lacombe[32] or of Kleintjens and Koningsveld.[33] LCSTs can be described within a Flory−Huggins incompressible lattice treatment by using a phenomenological temperature-dependent χ parameter. It is essential, however, to include a treatment of the compressibility of the fluid to investigate the underlying physical nature of the LCST in polymer systems in which the fluid phase behavior is driven solely by the solvent−polymer size asymmetry.[13,14] To our knowledge, no such study has been made in the investigation of the LCST phase behavior of aqueous solutions of PEG. The only study of compressibility effects (or pressure effects) in water + PEG mixtures is that by Bekiranov et al.,[34] who extended the model of Matsuyama and Tanaka[29] by introducing a pressure dependence for the number of solvent molecules attached to PEO (based on a preferred hydrogen-bonding volume[35]); however, the underlying model is still an incompressible lattice. As in the studies mentioned earlier, Bekiranov et al. are able to capture the closed-loop region of liquid−liquid immiscibility semiquantitatively for a range of PEO molecular weights. Bekiranov et al.[34] also examined the high-pressure phase data of water + PEO-270 000[9] by introducing an additional adjustable parameter to reproduce the high-pressure behavior reported experimentally: a second (re-entrant) homogeneous fluid region is predicted in this way with decreasing temperature.

In this paper we employ a continuum approach to investigate the phase behavior of the water + PEG mixture: the statistical associating fluid theory for potentials of variable range (SAFT-VR).[36,37] In contrast with lattice approaches, the use of a continuum treatment allows us to incorporate the effect of pressure in a rigorous fashion. The SAFT approach is also particularly well suited to the study of water-soluble polymers as both the polymer−solvent size asymmetry and hydrogen bonding can be accounted for explicitly. In the SAFT-VR equation of state, molecules are modeled as chains of spherical monomeric square-well segments; each segment is characterized by size (diameter) and dispersive energy (well depth and range) parameters. Hydrogen-bonding interactions are also taken into account by placing additional short-ranged bonding sites on the molecule, characterized by associative energy (well depth and range) parameters. At this stage we should also mention that the closely related soft-SAFT equation of state,[38,39] in which the chain molecules are formed from Lennard-Jones monomer segments, has been used to investigate the pressure−composition (weight fraction) representation of the vapor−liquid equilibrium (VLE) for mixtures of water + PEG-200 and water + PEG-6000.[40] The model was developed on the basis of previous studies of the ethylene glycol oligomer series[41] and involves molecular-weight-dependent interaction parameters. Unusually for a model of PEG in aqueous solution, however, hydrogen bonding between the polymer ether groups and water was neglected in this particular study. Though the VLE clearly appears not to be very sensitive to the unlike association, the effect of water−PEG hydrogen bonding (and solvation/hydration) on the LLE of such systems has been shown to be significant from various perspectives including experiment,[42–49] simulation,[18,50,51] and theory.[29–31,34,52,53]

Here we use a previously published[54] model of water, which provides an accurate description of the vapor−liquid equilibria and degree of association of pure water over a large temperature range (the triple point to ~90% of the critical point), and develop a model of PEG based on the hydroxyl (OH) end groups and the ethylene oxide (EO) repeat unit, following the methodology developed for the related alkyl polyoxyethylene surfactant $H-[CH_2]_n-[O-CH_2-CH_2]_m-OH$.[16] We account for the water−water and PEG−PEG like hydrogen-bonding interactions as well as the water−ether and water−hydroxyl unlike hydrogen bonding. All of the intermolecular potential parameters are temperature (state) independent and transferable, with a linear relationship between the number n of repeat units in the polymer and its molecular weight. Using these models, we investigate the characteristic closed-loop regions of liquid−liquid immiscibility for aqueous solutions of PEG ranging in molecular weight from PEG-2180 to PEG-1 020 000 and predict the complete pressure−temperature−composition ($P-T-w$) surface of the fluid phase equilibria of water + PEG-2180 and water + PEG-21 200. Of particular interest is the investigation of the high-pressure fluid phase behavior and its dependence on the molecular weight of the PEG polymer; hourglass regions of liquid−liquid immiscibility suggest high-pressure re-entrant phase behavior in such systems.

2. Models and Theory

2.1. Water. We use a Wertheim model of water recently proposed[54] (see Figure 1). This model has been shown to provide a good description of the thermodynamics, fluid phase equilibria, and degree of association of water within the SAFT-VR approach. The molecule is modeled as a single spherical square-well segment of hard-core diameter σ_{11}; the square well is characterized by a depth ϵ_{11} and a range λ_{11}. Four additional off-center square-well associating sites are used to mediate the hydrogen bonding. Two e sites represent the electronegative oxygen atom (the two lone pairs of electrons), and two H sites represent the hydrogen atoms. Only e−H bonding is permitted, allowing for up to two hydrogen bonds per water molecule, since a donor hydrogen or acceptor lone pair of electrons contributes half of a hydrogen bond. The sites are all placed at

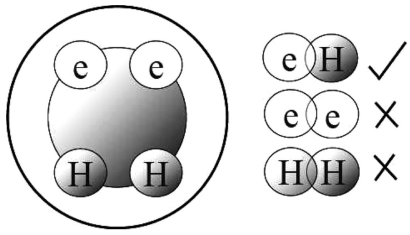

Figure 1. Model of water[54] used in the SAFT-VR studies of the fluid phase equilibria of aqueous solutions of PEG. The molecule is represented by a square-well core of diameter σ_{11} with dispersive interactions characterized by a well depth ϵ_{11} and a range λ_{11}. The hydrogen-bonding interactions are mediated through four off-center square-well bonding sites of types e (electron lone pairs) and H (hydrogen) located halfway between the center and surface of the molecular core; only e−H bonding is considered, and multiple bonding at a given site is forbidden. When an e and an H site come within a cutoff range $r^{HB}_{c,11,eH}$ of each other, there is a site−site hydrogen-bonding associative interaction of energy $\epsilon^{HB}_{11,eH}$.

Table 1. Pure Component Parameter Values for the Model of Water (Figure 1)[54] [a]

σ_{11}/Å	(ϵ_{11}/k)/K	λ_{11}	$(\epsilon^{HB}_{11,eH}/k)$/K	$r^{HB}_{c,11,eH}$/Å	$K^{HB}_{11,eH}$/Å^3
3.034 20	250.000	1.788 90	1400.00	2.108 22	1.066 73

[a] The parameters characterising the model are the diameter of the spherical core σ_{11}, the depth ϵ_{11}, and range λ_{11} of the dispersive square well, and the depth $\epsilon^{HB}_{11,eH}/k$ and the range $r^{HB}_{c,11,eH}$ (corresponding to the bonding volume $K^{HB}_{11,eH}$) of the hydrogen-bonding site−site interaction; the water molecule is treated as spherical, i.e., $m = 1$.

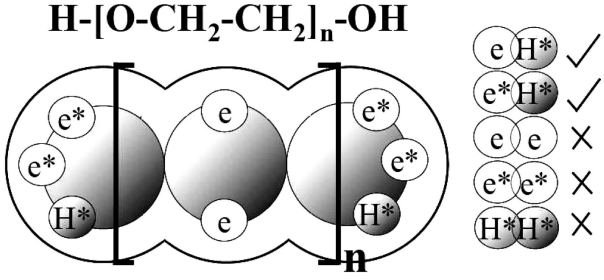

Figure 2. Model of PEG used in SAFT-VR studies of the fluid phase equilibria of aqueous solutions of PEG. The molecule is represented by a number m of square-well segments of diameter σ_{22} with dispersive interactions characterized by a well depth ϵ_{22} and a range λ_{22}. The hydrogen-bonding interactions are mediated through off-center square-well bonding sites of types e (ethylene oxide EO repeat unit oxygen electron lone pairs), e* (hydroxyl OH terminal oxygen electron lone pairs), and H* (hydroxyl OH terminal hydrogen atoms) located halfway between the center and surface of the segment core; only e−H* and e*−H* bonding is considered, and multiple bonding at a given site is forbidden. When a site e or e* and a site H* come within a cutoff range $r^{HB}_{c,22} = r^{HB}_{c,22,eH^*} = r^{HB}_{c,22,e^*H^*}$ of each other, there is a site−site hydrogen-bonding associative interaction of energy $\epsilon^{HB}_{22} = \epsilon^{HB}_{22,eH^*} = \epsilon^{HB}_{22,e^*H^*}$.

a distance $r^{HB}_{d,11}$ from the center of the sphere, and the cutoff range between the e and H sites is given by $r^{HB}_{c,11,eH}$. These two parameters define the volume $K^{HB}_{11,eH}$ available for e−H site−site bonding association.[55] When two sites of different water molecules are within a distance of $r^{HB}_{c,11,eH}$, they interact with an energy $\epsilon^{HB}_{11,eH}$. See Table 1 for a list of parameter values.

2.2. Poly(ethylene glycol) (PEG). The PEG (H−[O−CH_2−CH_2]$_n$−OH) chain is modeled as a number n of ethylene oxide (ethoxy) repeat units (monomers), with a hydroxyl group terminating each end of the polymer (see Figure 2). Traditionally, pure component parameters are obtained by optimizing the description of experimental pure-component phase equilibrium data, but for polymers there is a lack of such data due to their immeasurably low vapor pressure. Instead, we concentrate on characterizing the repeat unit of the polymer −[O−CH_2−CH_2]$_n$− as a number of square-well spherical segments m (aspect ratio) of hard-core diameter σ_{22}, square-well depth ϵ_{22}, and range λ_{22} from an examination of smaller oligomers and experimental data of their mixtures in water. A simple linear relationship between m and n allows one to describe PEG polymers of any molecular weight. Similar approaches to describe pure components have been employed for various homologous series,[56–58] including PEG[40] and the related alkyl polyoxyethylene surfactants.[8,16]

Modeling the repeat unit using aqueous mixtures of the ethylene glycol oligomer series may at first glance seem appealing, but for molecular weights $\lesssim$ 2140 g/mol PEG is completely soluble in water,[5] and there is therefore no liquid−liquid equilibria data for use in characterizing the binary mixture interactions. Both the polymer ethoxy repeat unit and hydroxyl end groups contribute to the solubility of PEG in water, as both are capable of hydrogen bonding with the solvent. For solutions of "high" molecular weight PEG this miscibility is governed by the ethylene oxide groups; the effect of the two hydroxyl end groups is insignificant in comparison with that of the large number of ether groups. For "low" molecular weight PEG the contribution of the hydroxyl groups becomes more significant and controls the miscibility of the polymer.[31,59] A parametrization based on the shorter ethylene glycol oligomers is expected to capture largely the contribution of the dominant hydroxyl groups and not the repeat ethoxy group of the molecule; the extrapolation of parameters based on a description of the phase equilibria of the shorter oligomers is unlikely to allow for a transferability of repeat-unit parameters with molecular weight. Instead, we consider the phase behavior of diethyl ether, DEE (CH_3−CH_2−O−CH_2−CH_3), and its mixtures with water to capture the characteristics of the ethylene oxide group; the intermolecular parameters of the ethoxy group are used to model the repeat unit −[O−CH_2−CH_2]− of PEG.

Diethyl ether is treated as nonassociating as far as its pure-component properties are concerned, as no hydrogen-bonding interactions are possible in the pure fluid. We model DEE as a homonuclear chain of m spherical segments, each of hard-core diameter σ_{22}, interacting via a square-well potential of depth ϵ_{22} and range λ_{22}. To obtain a value of m for DEE, we use an empirical relationship of the type[56]

$$m = \frac{N_a - 1}{3} + 1 \tag{1}$$

where N_a is the number of carbon and oxygen atoms in the backbone of the molecule. This relationship reduces to $m = 1$ for essentially spherical molecules such as methane or water and has been used to study the alkyl polyoxyethylene C_iE_j series with the SAFT-HS approach;[8,16] we should note that the C_iE_j models cannot be employed in our current study of PEG because they were developed for a mean-field version of SAFT[60–62] corresponding to a more primitive augmented van der Waals treatment (see, e.g., ref 63). The other intermolecular potential model parameters of DEE are determined by minimizing a relative least-squares objective function consisting of the sum of appropriate residuals for the vapor pressure p_v and saturated liquid density ρ_l:

$$\min_{(\sigma,\epsilon,\lambda)} F_{obj} = \sum_i \left[\frac{p^{exp}_{v,i} - p^{calc}_{v,i}(m,\sigma,\epsilon,\lambda)}{p^{exp}_{v,i}}\right]^2 + \sum_j \left[\frac{\rho^{exp}_{l,j} - \rho^{calc}_{l,j}(m,\sigma,\epsilon,\lambda)}{\rho^{exp}_{l,j}}\right]^2 \tag{2}$$

using a combined annealing and simplex technique.[64] We use 49 saturated liquid density and vapor pressure experimental data points,[65] ranging from the triple-point temperature T_t to 90% of the critical point $T/T_c = 0.90$. This upper cutoff in temperature

Table 2. Pure Component Parameter Values for the Model of Diethyl Ether (DEE) and Poly(ethylene glycol) (PEG) (Figure 2)[a]

model	m	σ_{22}/Å	(ϵ_{22}/k)/K	λ_{22}	(ϵ_{22}^{HB}/k)/K	$r_{c,22}^{HB}$/Å	K_{22}^{HB}/Å^3
DEE	2.333 33	3.812 39	287.601	1.461 89			
PEG	eq 3	3.812 39	287.601	1.461 89	1000.00	3.200 00	10.881 61

[a] The parameters characterizing the models are the number of segments in the chain m, the diameter of the spherical core σ_{22}, the depth ϵ_{22}, and range λ_{22} of the dispersive square well. For PEG molecules hydrogen bonding can take place between the lone pairs of electrons on the oxygen atoms of the repeat ethylene oxide unit or of the hydroxyl group and the hydrogen atoms of the hydroxyl group (EO−OH and OH−OH bonding), characterized by the strength $\epsilon_{22}^{HB} = \epsilon_{22,eH^*}^{HB} = \epsilon_{22,e^*H^*}^{HB}$ of the hydrogen-bonding site−site interaction, and the range $r_{c,22}^{HB} = r_{c,22,eH^*}^{HB} = r_{c,22,e^*H^*}^{HB}$ (corresponding to the bonding volume K_{22}^{HB}) of the site−site interaction.

was chosen to avoid including critical and near-critical data in the estimation, as this region is known to be poorly represented with analytical equations of state such as SAFT. To describe the critical region adequately, one would need to employ a renormalization group or crossover treatment, which is beyond the scope of our work. Once the optimal parameters are determined in this way, the number of segments m in the model and the square-well range λ_{22} are fixed, as they capture the nonconformal nature of the interactions in the fluid, while the conformal parameters σ_{22} and ϵ_{22} are rescaled to give the best description of the mixture at ambient conditions, where the liquid−liquid region is well characterized experimentally for the water + DEE mixture; in particular, the boiling point of DEE was used. This refinement ensures that the model of DEE correctly captures the water + DEE liquid−liquid coexistence phase behavior, the feature of interest in the phase behavior of water + PEG. The final set of parameters developed in this way is presented in Table 2; these are also used in a transferable way to model the ethoxy repeat unit of PEG (cf. Table 2).

The number of spherical segments of the model PEG chain is determined following a simplified version of eq 1. By assigning $N_a = 3n + 1$, where $3n$ corresponds to the number of atoms in the backbone of the polymer (two carbon and one oxygen in each repeat unit n) with an additional oxygen atom corresponding to the terminal hydroxyl group (note that the other terminal hydroxyl group is already included in the number of atoms in the backbone of the polymer obtained from the number of repeat units), eq 1 simplifies to

$$m = n + 1 \tag{3}$$

The relationship between the molecular weight of PEG MW^{PEG} and the number of repeat units n (and therefore the number of spherical segments m) is given by

$$MW^{PEG}/(g/mol) = 44n + 18 \tag{4}$$

where 44 g/mol is the molecular weight of the repeat ethylene oxide unit $-[CH_2-CH_2-O]-$ and 18 g/mol is the molecular weight of the OH− and the −H atom of the first and terminal hydroxyl groups.

As mentioned earlier, DEE is treated as a nonassociating molecule. In PEG, however, hydrogen bonding may occur between the hydrogen and oxygen atoms of the terminal hydroxyl groups (OH−OH bonding) as well as the hydrogen atoms of the hydroxyl groups and the oxygen atoms of the ether groups of the backbone (OH−EO bonding). The likelihood of OH−OH (or even OH−EO) hydrogen bonding is however debatable. Rayleigh wing and Fourier transform infrared spectroscopic studies[66] on PEG-200 and PEG-2000 suggest that OH−OH hydrogen bonding does not occur appreciably, while a 90 K difference in the phase boundary is found for mixtures with different end-group terminations in small-angle neutron scattering (SANS) and cloud-point measurements[67] of polystyrene−PEO blends for methoxy- and dimethoxy-terminated PEO-2000. A related SANS study for aqueous solutions of PEO ($w_{PEO} = 0.04$) suggests that for hydroxyl-terminated PEO the hydroxyl group(s) stay dissolved in water, whereas for methyl-terminated PEO, the methyl groups "stick" to the ethylene groups of PEO, creating branched and aggregated structures.[68] This suggests that for PEG no end-group association occurs while for PEO a type of "hydrophobic" interaction may occur. In a recent theoretical investigation with a Flory−Huggins approach,[31] in which hydrogen bonding was explicitly taken into account, OH−OH and OH−EO hydrogen bonding was reported as only noticeable at high volume fractions of PEO for a water−PEO-220 mixture. In our study we also include attractive short-ranged sites to allow for the possibility of both OH−OH and OH−EO hydrogen bonding on the basis that both are physically possible and require no extra cost in our calculations. One should note that the presence of sites in a particular model does not necessarily lead to bonding at any given site but to the possibility that an interaction of hydrogen-bonding type can occur; the probability of site−site bonding depends on the temperature and the site number density (which will necessarily be very low in the case of the OH−OH hydrogen bonding for high molecular weight PEG).

In view of the preceding discussion, a number of off-center square-well associating sites are used to mediate the like hydrogen bonding between PEG chains: two e* sites and one H* site are used to represent the electronegative oxygen atom (two lone pairs of electrons) and the hydrogen atom of a hydroxyl group (note that we consider two hydroxyl groups per PEG molecule), and two e sites per ethoxy repeat unit −EO− are used to represent the electronegative oxygen atom of the ether group. Only e*−H* and e−H* bonding is allowed, allowing for up to one and a half hydrogen bonds per hydroxyl group and one hydrogen bond per ether group. The sites are all placed at a distance $r_{d,22}^{HB} = 0.25\sigma_{22}$ from the center of a segment. For simplicity both the e*−H* and e−H* interactions are assumed to be equivalent, and therefore the cutoff range between two sites is given by $r_{c,22}^{HB} = r_{c,22,e^*H^*}^{HB} = r_{c,22,eH^*}^{HB}$. The values of $r_{d,22}^{HB}$ and $r_{c,22}^{HB}$ define the volume K_{22}^{HB} available for site−site bonding association.[55] When two sites are within a distance of $r_{c,22}^{HB}$, they interact with an energy $\epsilon_{22}^{HB} = \epsilon_{22,e^*H^*}^{HB} = \epsilon_{22,eH^*}^{HB}$. Optimized values for $r_{c,22}^{HB}$ (and therefore, K_{22}^{HB}) and ϵ_{22}^{HB} are obtained by comparison to experimental mixture data at the same time as the unlike binary parameters are determined, as described in the following section. The optimized intermolecular model parameters for PEG are presented in Table 2.

2.3. Unlike Binary Interaction Parameters. In order to model the phase behavior of the mixtures of interest, a number of unlike, or cross, binary intermolecular interaction parameters also need to be determined. Experimental[42–49,59] and simulation[18,50,51] studies confirm the formation of hydrogen bonds between water molecules and the ethylene oxide groups of PEG (water−EO) as well as between water and the terminal hydroxyl groups of PEG (water−OH). In our model this intermolecular association is mediated via the short-ranged association sites of the pure components. We are mostly interested in the closed-loop behavior of these systems, and so we have used the liquid−liquid equilibria data of Saeki et al.[5] and Bae et al.[69] for water + PEG mixtures of molecular weight 2180, 8000, and 21 200 g/mol (see Figure 3) as the reference data to determine all of the unlike intermolecular model parameters.

The unlike hydrogen-bonding parameters for the interaction between water and the PEG OH group are given by $r_{c,12^*}^{HB} = r_{c,12,eH^*}^{HB} = r_{c,12,He^*}^{HB}$, where both $r_{d,12}^{HB}$ and $r_{c,12^*}^{HB}$ define $K_{12^*}^{HB}$. The value of $r_{c,12^*}^{HB}$ is

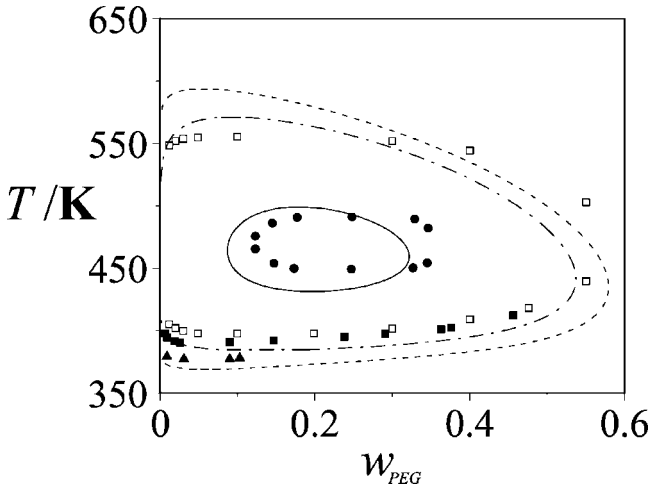

Figure 3. Temperature−composition (weight fraction) $T-w$ closed-loop regions of liquid−liquid immiscibility for aqueous solutions of PEG. The symbols correspond to experimental data at pressures along the three-phase line for PEG molecular weights of 2180[5] (●), 8000[5,69] (■, □), and 21 200[5] (▲) g/mol. The continuous curve, dot-dashed curve, and dashed curve correspond to the SAFT-VR description with the parameters defined in Tables 1–3 for PEG molecular weights of 2180, 8000, and 21 200 g/mol, respectively.

determined from an analysis of experimental mixture LLE data, while we set $r_{d,12}^{HB} = 0.25\sigma_{12}$. When a site on the water molecule (e or H) is within a distance of $r_{c,12^*}^{HB}$ of a site on the PEG chain (H* or e*), they interact with an energy of $\epsilon_{12^*}^{HB} = \epsilon_{12,eH^*}^{HB} = \epsilon_{12,He^*}^{HB}$. In the case of the association of water and the PEG ether group the unlike hydrogen-bonding parameters are characterized by $r_{c,12,He}^{HB}$, where the position $r_{d,12}^{HB}$ and range $r_{c,12,He}^{HB}$ define the bonding volume $K_{12,He}^{HB}$; when an H site on a water molecule is within a distance of $r_{c,12,He}^{HB}$ of an e site of the PEG ethoxy group, they interact with an energy of $\epsilon_{12,He}^{HB}$.

In addition to the determination of the unlike hydrogen-bonding model parameters, standard combining rules are used to obtain the unlike parameters characterizing the unlike repulsion and the range of the dispersive attractive interaction.[37] The arithmetic mean (Lorentz rule) is used for unlike diameter [$\sigma_{12} = (\sigma_{11} + \sigma_{22})/2$]; note that this relation is exact since the segments are modeled as hard repulsive cores. The range of the unlike water−PEG square-well dispersive attractive interaction is also described in terms of a simple arithmetic average [$\lambda_{12}\sigma_{12} = (\lambda\sigma_{11} + \lambda\sigma_{22})/2$].[37] The energy of the unlike dispersive attractive interaction is given by $\epsilon_{12} = (1 - k_{12})(\epsilon_{11}\epsilon_{22})^{1/2}$, where k_{12} is adjusted to provide the best description of the mixture liquid−liquid equilibria data; the binary interaction parameter k_{12} provides a measure of the deviation from the Berthelot rule (for a discussion of the physical significance of these relationships the reader is directed to ref 70). A full list of the water−PEG(EO) and water−PEG(OH) unlike interaction parameters is given in Table 3.

The equation of state of association models of the type that have been discussed here can be developed in a straightforward manner within the statistical associating fluid theory (SAFT) framework.[71,72]

2.4. The SAFT Equation of State. In this study we use the particular extension of SAFT for potentials of variable range (SAFT-VR)[36,37] to obtain the thermodynamic properties of our systems for the models described in the previous sections. The Helmholtz free energy A of our two-component associating fluid can be written in the usual SAFT form as

$$\frac{A}{NkT} = \frac{A^{\mathrm{IDEAL}}}{NkT} + \frac{A^{\mathrm{MONO}}}{NkT} + \frac{A^{\mathrm{CHAIN}}}{NkT} + \frac{A^{\mathrm{ASSOC}}}{NkT} \tag{5}$$

where N is the number of molecules, k is the Boltzmann constant, and T is the temperature. The term A^{IDEAL} corresponds to the ideal free energy of the mixture, and A^{MONO}, A^{CHAIN}, and A^{ASSOC} are residual contributions to the free energy due to monomer−monomer segment−segment repulsive and attractive (dispersion) interactions, to the formation of polymer chains, and to site−site intermolecular association (hydrogen bonding), respectively.

In the SAFT-VR approach the square-well monomer dispersive contribution for all the segments in the mixture is obtained from a Barker−Henderson[73,74] high-temperature perturbation expansion up to second order, i.e.

$$\frac{A^{\mathrm{MONO}}}{NkT} = \sum_{i=1}^{2} x_i m_i \left(\frac{A^{\mathrm{HS}}}{N_s kT} + \frac{A_1}{N_s kT} + \frac{A_2}{N_s kT} \right) \tag{6}$$

where x_i is the mole fraction of component i, m_i is the number of spherical segments that make up that component, and N_s is the total number of segments. The hard-sphere reference free energy A^{HS} is obtained from the expressions of Boublík[75] and Mansoori et al.[76] The mean attractive energy A_1 can be expressed analytically by an appropriate mapping where the contact value of the radial distribution function at an effective density is used in place of the integral over the radial distribution function. The second-order term A_2 is treated within the local compressibility approximation.[73,74,77]

The residual contribution to the free energy due to the formation of chain molecules is given in terms of the contact value of the pair distribution function $g_{ii}(\sigma_{ii})$ of the monomer reference fluid[78]

$$\frac{A^{\mathrm{CHAIN}}}{NkT} = -\sum_{i=1}^{2} x_i (m_i - 1) \ln g_{ii}^{SW}(\sigma_{ii}) \tag{7}$$

where $g_{ii}^{SW}(\sigma_{ii})$ is also obtained from a high-temperature expansion.

The residual contribution to the free energy due to association takes the form[55,78]

$$\frac{A^{\mathrm{ASSOC}}}{NkT} = \sum_{i=1}^{2} x_i \left[\sum_{a=1}^{s_i} \left(\ln X_{i,a} - \frac{X_{i,a}}{2} \right) + \frac{s_i}{2} \right] \tag{8}$$

where s_i is the total number of sites on a molecule of species i and $X_{i,a}$ is the fraction of molecules of species i not bonded at site of type a. The specific expression for the model water (1) + PEG (2) system described in the previous sections is shown explicitly below

$$\begin{aligned} \frac{A^{\mathrm{ASSOC}}}{NkT} = {} & x_1 \left[2\left(\ln X_{1H} - \frac{X_{1H}}{2} \right) + 2\left(\ln X_{1e} - \frac{X_{1e}}{2} \right) + 2 \right] + \\ & x_2 \left[2(n-1)\left(\ln X_{2e} - \frac{X_{2e}}{2} \right) + 4\left(\ln X_{2e^*} - \frac{X_{2e^*}}{2} \right) + \right. \\ & \left. 2\left(\ln X_{2H^*} - \frac{X_{2H^*}}{2} \right) + n + 2 \right] \end{aligned} \tag{9}$$

where we recall that n is the number of repeat ethylene oxide units (EO) in the polymer molecule. Since one hydroxyl group is included at each end of the PEG polymer, there are actually 2 (n − 1) ether e sites, 4 hydroxyl e* sites, and 2 hydroxyl H* sites (see Figure 2). The degree of association at each site is quantified by $X_{i,a}$, which is obtained from the mass action equation[78] as

$$X_{i,a} = \frac{1}{1 + \sum_{j=1} \sum_{b=1} \rho x_j X_{j,b} \Delta_{ij,ab}} \tag{10}$$

where $\rho = N/V$ is the number density of the fluid and $X_{j,b}$ is the fractionof molecules not bonded at a site of type b. The function $\Delta_{ij,ab}$ depends on the contact value $g^{SW}(\sigma_{ij})$ of the radial distribution function of the monomer fluid (a square-well

Table 3. Unlike (Binary) Interaction Parameter Values for the Water−PEG and Water−DEE Segment Dispersion Interaction k_{12} and Water−Ethylene Oxide (Water−EO) Hydrogen Bonding (Characterized by a Strength $\epsilon^{HB}_{12,He}$ and Range $r^{HB}_{c,12,He}$, Corresponding to $K^{HB}_{12,He}$) for Poly(ethylene glycol) (PEG) (Figure 2) and Diethyl Ether (DEE)[a]

system	k_{12}	$(\epsilon^{HB}_{12,He}/k)$/K	$r^{HB}_{c,12,He}$	$K^{HB}_{12,He}$/Å^3	(ϵ^{HB}_{12}/k)/K	$r^{HB}_{c,12}$/Å	K^{HB}_{12}/Å^3
water−PEG	−0.053	1505.00	2.188 00	0.529 02	2320.00	2.188 00	0.529 02
water−DEE; opt	−0.150	800.000	2.378 57	1.532 00			
water−DEE; trans	−0.053	1505.00	2.188 00	0.529 02			

[a] The top set of water−DEE parameters (opt) correspond to the parameters optimised by refinement to the $T-x$ phase diagram at a pressure of 0.101 MPa, and the second set correspond to the transferable (trans) parameters used to describe the water−PEG mixtures. In the case of aqueous solutions of PEG, hydrogen bonding is also possible between water and the terminal hydroxyl groups of PEG; this water−OH association is characterized by a strength $\epsilon^{HB}_{12} = \epsilon^{HB}_{12,eH^*} = \epsilon^{HB}_{12,He^*}$ and range $r^{HB}_{c,12^*} = r^{HB}_{c,12,eH^*} = r^{HB}_{c,12,He^*}$ (corresponding to K^{HB}_{12}) (cf. Figure 2).

reference fluid), the Mayer function $f_{ij,ab} = \exp(\epsilon_{ij,ab}/kT) - 1$ of the site−site hydrogen-bonding interaction (characterized by a square well of depth $-\epsilon_{ij,ab}$), and the site−site bonding volume $K^{HB}_{ij,ab}$:

$$\Delta_{ij,ab} = K^{HB}_{ij,ab} f_{ij,ab} g^{SW}(\sigma_{ij}) \tag{11}$$

The relation between the reduced position $r^*_{d,ij} = r_{d,ij}/\sigma_{ij}$ and range $r^*_c = r_{c,ij,ab}/\sigma_{ij}$ of the site−site interaction; and the reduced bonding volume $K^*_{ij,ab} = K^{HB}_{ij,ab}/\sigma_{ij}^3$ for square-well bonding sites is given by[55]

$$K^*_{ij,ab} = 4\pi[\ln(r^*_c + 2r^*_d)(6r^{*3}_c + 18r^{*2}_c r^*_d - 24r^{*3}_d) + (r^*_c + 2r^*_d - 1) \times (22r^{*2}_d - 5r^*_c r^*_d - 7r^*_d - 8r^{*2}_c + r^*_c + 1)]/(72r^{*2}_d) \tag{12}$$

Though the degree of hydrogen bonding in the system is fully characterized by the strength of the site−site interaction and the overall bonding volume, it is often more convenient and physically intuitive to describe the volume accessible to bonding in terms of the range parameter r^*_c.

For the water + PEG mixture, the fractions of molecules not bonded at given sites are obtained from eq 10 as

$$X_{1e} = \frac{1}{1 + 2\rho x_1 X_{1H}\Delta_{11,eH} + 2\rho x_2 X_{2H^*}\Delta_{12^*}} \tag{13}$$

for the fraction of water molecules not bonded at a site of type e

$$X_{1H} = \frac{1}{1 + 2\rho x_1 X_{1e}\Delta_{11,eH} + 2(n-1)\rho x_2 X_{2e}\Delta_{12,He} + 4\rho x_2 X_{2e^*}\Delta_{12^*}} \tag{14}$$

for the fraction of water molecules not bonded at a site of type H

$$X_{2e} = \frac{1}{1 + 2\rho x_1 X_{1H}\Delta_{12,He} + 2\rho x_2 X_{2H^*}\Delta_{22}} \tag{15}$$

for the fraction of PEG molecules not bonded at a site of type e (on the ether oxygen)

$$X_{2e^*} = \frac{1}{1 + 2\rho x_1 X_{1H}\Delta_{12^*} + 2\rho x_2 X_{2H^*}\Delta_{22}} \tag{16}$$

for the fraction of PEG molecules not bonded at a site of type e* (the hydroxyl oxygen), and

$$X_{2H^*} = \frac{1}{1 + 2\rho x_1 X_{1e}\Delta_{12^*} + 2(n-1)\rho x_2 X_{2e}\Delta_{22} + 4\rho x_2 X_{2e^*}\Delta_{22}} \tag{17}$$

for the fraction of molecules not bonded at a site of type H* on the PEG molecule (the hydroxyl hydrogen). The association parameter $\Delta_{ij,ab}$ (which defines the different types of hydrogen bonding) is of four different types: $\Delta_{11,eH}$ characterizes the association between the e and H sites of the water molecules; $\Delta_{22} = \Delta_{22,eH^*} = \Delta_{22,e^*H^*}$ the association between the hydroxyl H* sites and the hydroxyl e* sites or ether e sites of PEG; $\Delta_{12,He}$ the association between the H sites of water and the ether e sites of PEG; $\Delta_{12^*} = \Delta_{12,eH^*} = \Delta_{12,He^*}$ the association between e or H sites of water and hydroxyl H* or e* sites of PEG. For a more detailed description of the individual terms of the SAFT-VR equation of state, we refer the reader to the original papers.[36,37]

The other thermodynamic properties can be obtained from the Helmholtz free energy using standard relationships: the pressure is obtained from the partial derivative of the free energy with respect to volume $p = -(\partial A/\partial V)_{\bar{N},T}$ (where $\bar{N}$ refers to the set of numbers of particles of all the components in the mixture), and the chemical potential from the partial derivative with the number of particles of each species $\mu_i = (\partial A/\partial N_i)_{V,T,N_j}$. The phase equilibria between two coexisting phases, α and β, require that the temperature, pressure, and chemical potential for each component i in each phase are equal, i.e., $T^\alpha = T^\beta$, $p^\alpha = p^\beta$, and $\mu^\alpha_i = \mu^\beta_i$ $(\forall i)$. The conditions for phase equilibria are employed to solve for the compositions and densities of the coexisting phases at a given temperature and pressure by using two different methods. We calculate the liquid−liquid equilibrium by first determining the spinodal composition roots based on the condition that $\partial^2 G_m/\partial x_i^2|_{p,T} = 0$, where G_m is the molar Gibbs free energy of the mixture for a specified temperature ($T^{spec} = T^\alpha = T^\beta$) and pressure ($p^{spec} = p^\alpha = p^\beta$). The particularly convenient expression of Kouskoumvekaki and von Solms for a binary system[79] for the second derivative of the Gibbs function

$$\left.\frac{\partial^2 G_m}{\partial x_1^2}\right|_{p,T} = \frac{1}{x_1 x_2}\left(1 - x_2 \left.\frac{\partial \bar{\mu}_2}{\partial x_1}\right|_{p,T}\right) \tag{18}$$

is used; in this approach the ideal contribution $(1/x_1x_2)$ is factored out to leave the composition derivative of the residual chemical potential $\bar{\mu}_2$. The compositions of the spinodal boundary of each phase $x_i^{s,\alpha}$ and $x_i^{s,\beta}$ are obtained from the solution of $x_2(\partial\bar{\mu}_2/\partial x_1|_{p,T}) - 1 = 0$; $\partial^2 G_m/\partial x_2^2|_{p,T}$ and the mixed derivative $\partial\bar{\mu}_1/\partial x_2|_{p,T}$ can be obtained in a similar fashion. At this point, we note that we are working in the Gibbs free energy space, where the natural thermodynamic variables are $\bar{N}$ (or $\bar{x}$), p, and T. The SAFT equation of state is, however, written in terms of the Helmholtz free energy where the natural variables are $\bar{N}$ (or $\bar{x}$), V, and T. In the calculation of the chemical potential $\mu_i(T^{spec}, V(p^{spec}), x_i)$ a pressure solver has to be used to determine the volume (density) roots corresponding to the chosen temperature, pressure, and composition. The binodal (coexistence) compositions are obtained by specifying an initial chemical potential for one component μ_1^* which is bounded by the spinodal chemical potentials, $\mu_1^{s,\alpha}(T^{spec}, V(p^{spec}), x_1^{s,\alpha})$ and $\mu_1^{s,\beta}(T^{spec}, V(p^{spec}), x_1^{s,\beta})$; the chemical potentials at the spinodal boundaries correspond to a maximum and a minimum in the chemical potential−composition curve between which the chemical potential at coexistence (binodal) must be found. At the binodal the following condition must be satisfied:

$$\mu_1^* = \mu_1^\alpha(T^{spec}, V(p^{spec}), x_1^\alpha) = \mu_1^\beta(T^{spec}, V(p^{spec}), x_1^\beta) \tag{19}$$

This relation is solved for a fixed μ_1^* to determine the compositions x_1^α and x_1^β of the two phases at which the chemical

potential of component 1 is equal. The chemical potential μ_1^* is then varied iteratively until the corresponding chemical potentials of the second component in each of the phases also satisfy the equilibrium condition

$$\mu_2^{\alpha}(T^{\text{spec}}, V(p^{\text{spec}}), x_1^{\alpha}(\mu_1^*)) = \mu_2^{\beta}(T^{\text{spec}}, V(p^{\text{spec}}), x_1^{\beta}(\mu_1^*)) \quad (20)$$

A root finding method known as the van Wijngaarden−Dekker−Brent method[64] (which combines bracketing, bisection and inverse quadratic interpolation) is used to obtain the binodal roots for the coexistence compositions $x_1^{b,\alpha}$ and $x_1^{b,\beta}$. This algorithm allows the solution of the liquid−liquid equilibrium compositions and densities at any pressure and temperature without the need for arbitrary initial guesses.

Unfortunately, in the regions of vapor–liquid equilibrium, far from critical conditions, the Gibbs surface becomes discontinuous as there can be up to three density roots under certain conditions; in this case the derivative of the Gibbs function (and thus the chemical potential) can become ill-defined, which causes difficulties with the numerical differentiation used in the calculation of spinodal composition. In these regions we solve the standard set of nonlinear equations corresponding to thermal, mechanical, and chemical equilibria

$$T^{\text{spec}} = T_i^{\alpha} = T_i^{\beta} \quad (21)$$

$$p^{\text{spec}} = p_i^{\alpha} = p_i^{\beta} \quad (22)$$

and

$$\mu_i^{\alpha} = \mu_i^{\beta}, \ \forall\, i \quad (23)$$

using the Levenberg−Marquardt method[64] with appropriate initial guesses of composition and density.

3. Results and Discussion

In this study we are interested in the phase behavior of aqueous PEG solutions in the liquid region with a particular focus on the closed-loop immiscibility exhibited by these systems. The use of an analytical molecular approach such as SAFT allows one to undertake a global investigation of the phase behavior of the mixtures. This means that one can examine wide ranges of temperature and pressure as well as of the molecular weight of the polymer. We have developed models that are fully transferable so that only the number of repeat units n corresponding to a given molecular weight of the polymer, which is reflected in the number of spherical segments m in our model chain molecules, is required as an input for each mixture. The other pure component and mixture parameters are summarized in Tables 1, 2, and 3 as indicated earlier.

3.1. Water + DEE. We have used DEE ($CH_3-CH_2-O-CH_2-CH_3$) to determine the parameters that characterize the dispersive attractive and repulsive interactions of the monomer segments of the PEG repeat unit ($-[CH_2-CH_2-O]-$). It is interesting to note that DEE is also the smallest "polymer" of the PEO series (where PEO as defined earlier is interpreted as the PEG polymer terminated with methyl groups rather than with hydroxyl groups). We therefore investigate the related phase behavior of the water−DEE mixture.

Though DEE does not hydrogen bond as a pure component, in aqueous solution hydrogen bonding is active between the hydrogen atoms of the water molecule and the lone pairs on the oxygen atom in the ether group of DEE. As for PEG, we introduce two off-center square-well associating sites of type e in the DEE model to mediate the unlike hydrogen bonding of DEE with water. The sites are again positioned at $r_{d;12}^{HB} = 0.25\sigma_{12}$ from the center of the segment. The volume available for the unlike hydrogen bonding is then characterized by $r_{c,12,He}^{HB}$, as both $r_{d,12}^{HB}$ and $r_{c,12,He}^{HB}$ define the bonding volume $K_{12,He}^{HB}$. When an H site in water and an e site in DEE are closer than a cutoff distance of $r_{c,12,He}^{HB}$ apart, a hydrogen-bonding energy $\epsilon_{12,He}^{HB}$ is realized. The parameters characterizing this hydrogen-bonding interaction, i.e., $r_{c;12,He}^{HB}$ (or $K_{12,He}^{HB}$), and the unlike dispersive attractive energy between water and DEE, characterized by the well depth ϵ_{12} of the corresponding square-well interaction or, alternatively, the binary interaction parameter k_{12}, can be obtained by either transferring the value optimized for the water−PEG interaction or by direct refinement to the experimental fluid phase equilibria data of the water + DEE mixture. The remaining unlike interaction parameters σ_{12} and λ_{12} are determined following standard combining rules as described earlier.

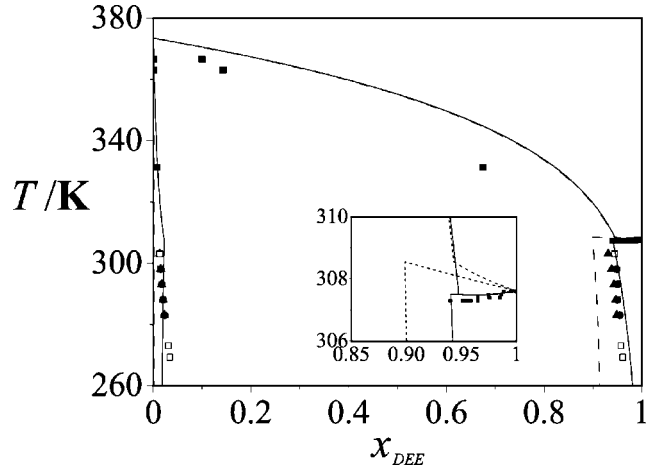

Figure 4. Temperature−composition $T-x$ fluid phase diagram of the water + DEE mixture at a pressure of 0.101 MPa. The symbols represent the experimental data of Borisova et al.[80] (■), Bennett and Philip[81] (●), Kablukov and Malischeva[82] (▲), and Hill[83] (□). The continuous curve is the SAFT-VR description obtained by refining the unlike interaction parameters. The dashed curve is the SAFT-VR prediction using the transferable water−PEG unlike interaction parameters (see Table 3).

We first chose to examine water−DEE experimental temperature−composition ($T-x$) slices of the fluid phase equilibria at 0.101 MPa to determine the unlike interaction parameters, as both liquid−liquid and vapor−liquid data are available at this pressure.[80–83] The water−DEE $T-x$ phase diagram at 0.101 MPa is shown in Figure 4. A broad region of liquid−liquid equilibrium (LLE) is seen to extend up to ∼307 K, at which point the system appears to exhibit a heteroazeotrope in the DEE-rich region. From the three-phase heteroazeotrope composition line, a region of vapor−liquid equilibrium (VLE) is seen to extend to ∼373 K (the boiling temperature of water). In the figure the description obtained with the SAFT-VR approach for our model water + DEE mixture are compared to the experimental data. Two sets of model parameters are examined (see Table 3): a transferable set of parameters that is also appropriate in studies of water + PEG mixtures and a set of optimized parameters for the water + DEE mixture. The region of LLE is well represented by both sets of model parameters; as one would expect, the extent of immiscibility is described more accurately when the water−DEE LLE data are used to refine the parameters. An excellent prediction of the heteroazeotrope (see inset of Figure 4) at ∼307 K is also obtained for the parameters which have been refined to the LLE data.

The complete pressure−temperature−composition ($P-T-x_{\text{DEE}}$) surface of the fluid phase diagram as obtained using the unlike parameters refined to the data at 0.101 MPa is shown in Figure 5. We find that the mixture exhibits type II phase behavior in the classification of van Konyenburg and Scott.[84] Two separate loci of critical points, a continuous gas−liquid

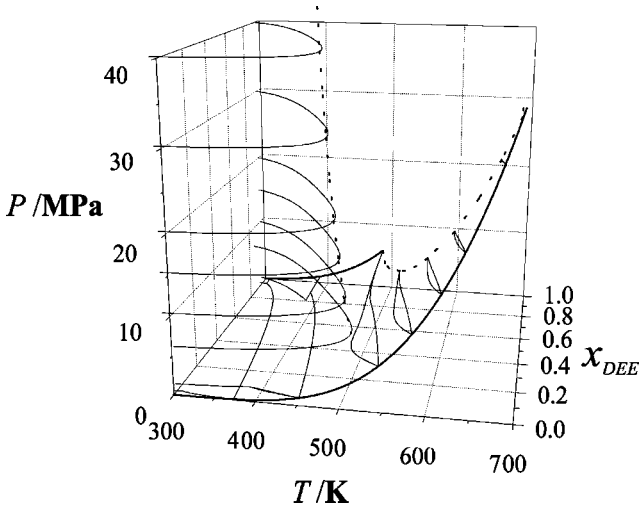

Figure 5. SAFT-VR prediction of the pressure−temperature−composition $P-T-x$ surface of the fluid phase diagram of water + DEE using the optimal unlike interaction parameters (see Table 3). The thick continuous curves represent the saturated vapor pressures of water and DEE. The thin black curves mark the regions of vapor−liquid and liquid−liquid immiscibility, and the dotted curves denote the critical lines.

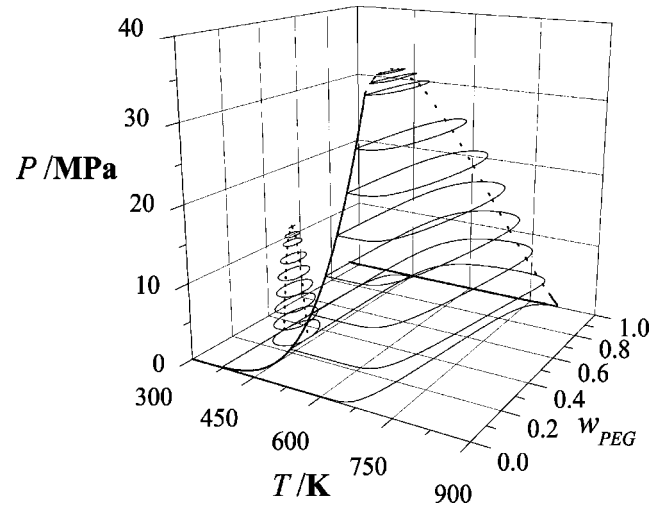

Figure 6. SAFT-VR prediction of the pressure−temperature−composition (weight fraction) $P-T-w$ surface of the fluid phase diagram for aqueous solutions of PEG with a molecular weight of 2180 g/mol. The thick continuous curves represent the saturated vapor pressures of water and PEG. The thin continuous curves mark the regions of vapor−liquid and liquid−liquid immiscibility, and the dotted curves denote the critical lines.

line and a liquid−liquid line, are clearly seen. We note that the corresponding phase diagram calculated with transferable parameters leads to type III phase behavior, with a continuous gas−liquid to liquid−liquid critical line at high temperatures and pressures. The latter model suggests a greater immiscibility between water and DEE (as seen in Figure 4) and as a result a change from type II to type III phase behavior.

3.2. Water + PEG. We have examined experimental data for the water + PEG system and have chosen to use the LLE data for PEG with molecular weights of 2180, 8000, and 21 200 g/mol to determine the unlike adjustable parameters of the model. The liquid region is of particular interest as the closed-loop liquid−liquid immiscibility exhibited by these mixtures is still the subject of much work and debate. Three molecular weights are selected over a wide range with the final aim of obtaining parameters that are representative of the smaller and larger polymers. The experimental and calculated closed-loop coexistence curves have already been presented in Figure 3 as a $T-w_{PEG}$ representation (where w_{PEG} is the weight fraction of PEG). One should note that experimental data such as those presented in the figure are typically obtained by heating solutions in sealed cells,[5,69] so that in fact one is determining the cloud point temperatures from the upper critical end point (UCEP) to the lower critical end points (LCEP) (see ref 85); as the temperature is increased in such a setup the pressure also increases, following the three-phase (orthobaric) line. In the SAFT calculations, therefore, the pressure of the three-phase VLLE line at the corresponding temperature is used to map out the LLE coexistence boundary. In the case of polymers of high molecular weight there are numerical difficulties in determining the three-phase line due to its very close proximity to the vapor pressure of the solvent (as will become clear later). Instead, it is more convenient, with virtually no loss of accuracy, to approximate the pressure of the three-phase coexistence by the vapor pressure of pure water at the corresponding temperature.

The aqueous solutions of PEG for the three selected molecular weights all exhibit the characteristic region of closed-loop liquid−liquid immiscibility: at low temperatures the mixtures are completely miscible; as the temperature is increased, a two-phase region may be obtained (depending on the total composition); and on further increase of temperature complete miscibility is again seen. A clear trend with molecular weight can also be observed, with the smallest loop (both in terms of the range of temperatures and of the range of composition) corresponding to the lowest molecular weight and the largest loop to the highest molecular weight polymer. As can be seen in the figure, the transferable set of intermolecular potential model parameters that have been developed (see Tables 1–3 for the specific parameter values) provides a very good description of the experimental LLE data. The calculated LCEPs and UCEPs are all within ∼5−15 K of the experimental values. It is noticeable that the lower critical temperatures are underpredicted by the SAFT-VR equation of state while the upper critical temperatures are overpredicted by the theory. This is to be expected since with a SAFT approach, as with all analytical equations of state, the critical region cannot be captured rigorously. Furthermore, the deviation in these regions is also comparable to the scatter in the experimental data; a difference of ∼8 K is observed between the experimental LCST data of Bae et al.[69] and of Saeki et al.[5] for the water + PEG-8000 mixture. This difference may be a consequence of differences in the polydispersity of the samples, an effect we have not thus far investigated. It is however very gratifying to find that the asymmetric shapes of the closed loops characteristic of the higher molecular weight PEG systems are reproduced by the theory.

The theory is then used to examine the global pressure−temperature−composition ($P-T-w_{PEG}$) fluid phase behavior of two of the mixtures. The $P-T-w_{PEG}$ surfaces for water + PEG-2180 and water + PEG-21 200 are presented in Figures 6 and 7, respectively. It is immediately clear that both mixtures exhibit type VI phase behavior within the van Konynenburg and Scott classification,[84] with a continuous gas−liquid critical line running between the critical point of the two pure components and a region of liquid−liquid immiscibility bounded below and above by a critical line which corresponds to the locus of the upper and lower critical solution temperatures. The liquid−liquid immiscibility is seen to disappear at a maximum in pressure (sometimes called a hypercritical point). A link has been made between the high-pressure denaturation of proteins and their increased miscibility in water with increasing pressure; the domelike immiscibility boundary of aqueous solutions of PEG (which are biocompatible polymers) and the complete miscibility seen beyond a hypercritical pressure are certainly consistent with this picture of protein denaturation.[86–90]

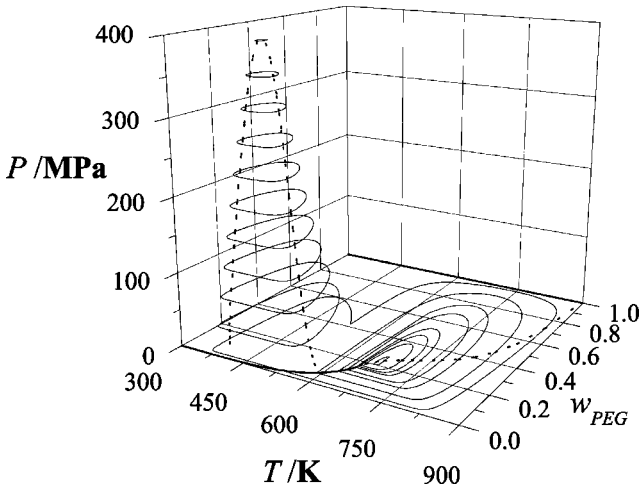

Figure 7. SAFT-VR prediction of the pressure−temperature−composition (weight fraction) $P-T-w$ surface of the fluid phase diagram for aqueous solutions of PEG with a molecular weight of 21 200 g/mol. The thick continuous curves represent the saturated vapor pressures of water and PEG. The thin continuous curves mark the regions of vapor−liquid and liquid−liquid immiscibility, and the dotted curves denote the critical lines.

In the case of the mixture with PEG-2180 (Figure 6), the closed-loop region of liquid−liquid immiscibility is seen to extend to pressures of ∼17.1 MPa. The vapor−liquid equilibrium region is very large in comparison, extending from the critical point of water toward that of the polymer, so that the liquid−liquid region appears somewhat dwarfed; most of the VLE region predicted in our calculations will not be accessible experimentally due to the thermal degradation of PEG at the higher temperatures. It should also be noted that the critical temperature and pressure of pure water and of PEG are overpredicted by the theory; the parameters of the two components would need to be rescaled to their critical points to provide a better description of the critical lines, but as we are primarily interested in the LLE region, this has not been done in our current study. The closed-loop region of liquid−liquid immiscibility for the water + PEG-21 200 system is seen to extend to a maximum pressure of ∼400 MPa, at which point the LCST and UCST meet at a hypercritical point. It is clear from the $P-T-w_{PEG}$ surface shown in Figure 7 that in this case the liquid−liquid region is the more extensive, with the vapor−liquid region dwarfed in pressure by comparison. The experimental data of Sun and King[10] for the water + PEG-21 200 mixture indicate that the LCST and UCST do not meet at a hypercritical point and that, instead, the region of liquid−liquid immiscibility becomes more extensive with increasing pressure. They report a turning point in the trend of the behavior of the LCSTs with pressure ∼550 MPa. Above this pressure a sharp decrease in the LCST is reported, while the more usual trend of a decrease in the LCST with decreasing pressure is reported below ∼550 MPa. An in-depth discussion of this high-pressure phase behavior will be left until the end of this section.

The extent of the VLE and LLE coexistence regions are more clearly seen in pressure−temperature ($P-T$) projections of the full phase surface. A comparison of the $P-T$ projections for the water + PEG-2180 and water + PEG-21 200 systems is given in Figure 8. The pressure along the three-phase vapor−liquid−liquid line (shown in the inset of Figure 8) is virtually indistinguishable to that of the vapor pressure of water, justifying our earlier methodology for computing the closed loops along the orthobaric line. The three-phase line for the water + PEG-2180 mixture is found to extend between a temperature of ∼432 and ∼495 K and a pressure of ∼0.6 and

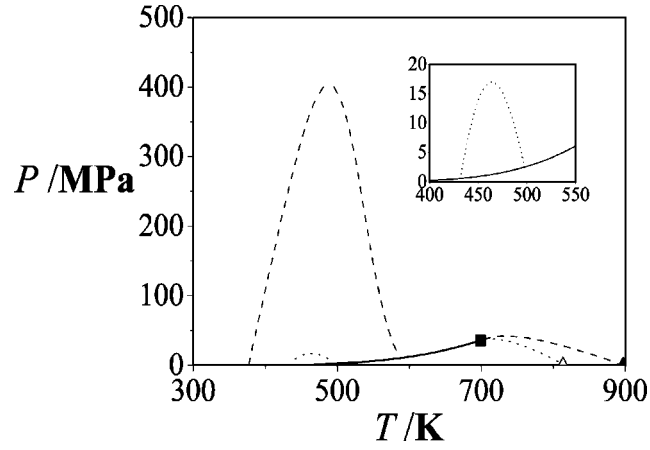

Figure 8. SAFT-VR prediction of the pressure−temperature $P-T$ projection of the fluid phase diagram of aqueous solutions of PEG with molecular weights of 2180 and 21 200 g/mol. The thick continuous curves represent the saturated vapor pressures of water (bounded by the critical point ■), PEG-2180 (bounded by △), and PEG-21 200 (bounded by ▲). The vapor−liquid and liquid−liquid critical lines for PEG-2180 and PEG-21 200 g/mol mixtures are denoted by the dotted curves and the dashed curves, respectively. The three-phase gas−liquid−liquid line for both systems are indistinguishable from the vapor pressure curve of pure water (see inset).

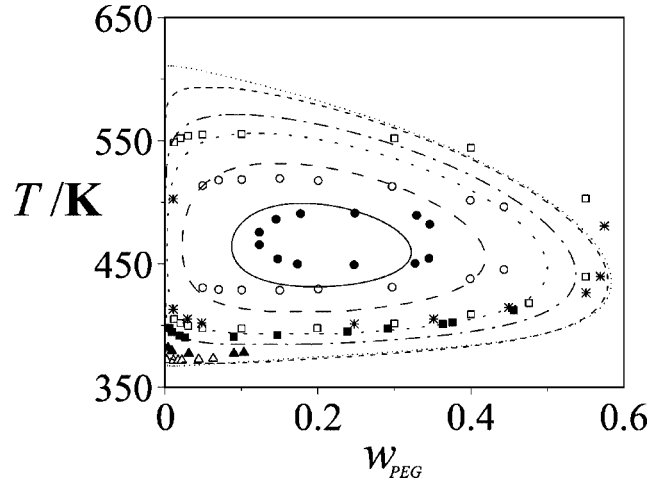

Figure 9. Temperature−composition (weight fraction) $T-w$ closed-loop regions of liquid−liquid immiscibility for the aqueous solutions of PEG. The symbols correspond to experimental data at pressures along the three-phase line for PEG molecular weights of 2180[5] (●), 3350[69] (○), 5000[2] (∗), 8000[5,69] (■, □), 21 200[5] (▲), and 1 020 000[5] (△) g/mol. The continuous, dashed, dotted, dot-dashed, dashed, and dotted curves from the inside to the outside correspond to the SAFT-VR description for PEG molecular weights of 2180, 3350, 5000, 8000, 21200, and 1 020 000 g/mol, respectively.

∼2.4 MPa. In the case of the water + PEG-21 000 mixture the three-phase line lies between temperatures of ∼377 and ∼588 K and pressures of ∼0.1 and ∼11 MPa. The large region of liquid−liquid immiscibility obtained for the aqueous solution of the higher molecular weight polymer is also clearly seen in this representation.

As an assessment of the transferability of the parameters in our model, we have calculated the closed-loop boundaries for a number of water + PEG binary mixtures of varying molecular weight and compared our predictions with the corresponding experimental data in Figure 9. The LLE experimental data of Malcolm and Rowlinson,[2] Saeki et al.,[5] and Bae et al.[69] which correspond to aqueous solutions of PEG with molecular weights of 2180, 3350, 5000, 8000, 21 200, and 1 020 000 g/mol are examined. As before, the closed-loop LLE is essentially

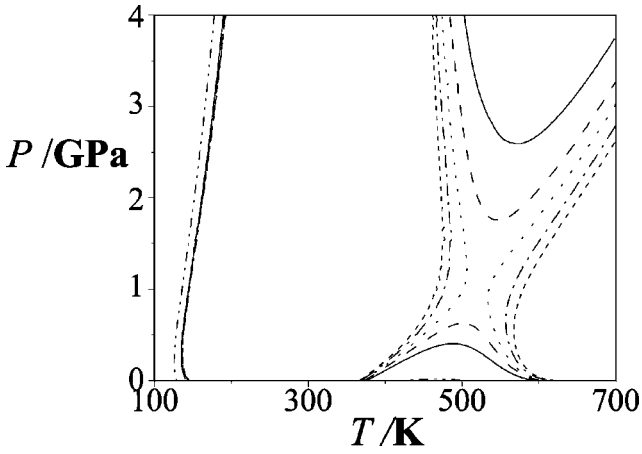

Figure 10. SAFT-VR prediction of the high-pressure $P-T$ projection of the fluid phase diagram of aqueous solutions of PEG. The dot-dot-dashed, continuous, dashed, dotted, dot-dashed, and short-dashed curves (from the inside to the outside) correspond to the liquid−liquid critical lines predicted with SAFT-VR for PEG molecular weights of 2180, 21 200, 50 000, 100 000, 270 000, and 1 020 000 g/mol.

computed along the three-phase line by approximating the orthobaric pressure by the vapor pressure of pure water. The varying pressure along the three-phase line should not be neglected as the pressure differences between the UCEP and LCEP become significant for high PEG molecular weights where the region of liquid−liquid immiscibility spans a large temperature range. For example, the difference in pressure between the UCEP and LCEP of the closed-loop LLE region for water + PEG-21 200 is ∼11 MPa. We can see that in general good agreement with the experimental data is obtained. This is very encouraging considering that we are using SAFT-VR to describe all of these complex associating systems with a single set of transferable intermolecular potential parameters. The width of the liquid−liquid immiscibility regions is in good agreement with experimental data, though a little underestimated at the higher temperatures of the polymer-rich phase. The LCST for all of our mixtures is slightly underestimated and the UCST slightly overestimated as expected with a standard analytical description of the free energy. When the molecular weight of PEG is increased, the region of liquid−liquid immiscibility becomes more extensive, so that the LCST is seen to move to lower temperatures and the UCST to higher temperatures. It is also clear that the LLE boundaries are predicted to converge in the region of the LCEP as the molecular weight of PEG is increased, a finding that is consistent with experimental observation. There is a difference of only ∼ 2K in the LCEP of the aqueous solutions of PEG-21 200 and PEG-1 020 000. The decrease in the LCST with increasing molecular weight is consistent with polymer-type behavior in which the liquid−liquid immiscibility is driven by the size asymmetry between the solvent and polymer molecules.[13] We leave a quantitative discussion of the thermodynamic drivers for this type of behavior for a future paper.[19]

Motivated by the unusual experimental phase behavior reported by Sun and King[10] and others,[9] we take advantage of the transferability of our models within the SAFT-VR approach to investigate the regions of very high pressures and low temperatures in aqueous solutions of PEG of varying molecular weight. Our predictions of the pressure−temperature behavior of the fluid phase equilibria over an extensive range of conditions are presented in Figure 10. For the water + PEG-21 000 mixture, in addition to the "lower" pressure region of liquid−liquid immiscibility extending to ∼400 MPa which was presented earlier in Figures 6 and 8, we find a region of high-pressure liquid−liquid immiscibility bounded by a lower hypercritical pressure at ∼2.6 GPa and 570 K. This type of high-pressure immiscibility has been observed in mixtures of 3-methylpyridine + H_2O + D_2O.[7] van Pelt et al.[91] also obtained this type of isolated high-pressure region of LLE in calculations for model binary mixtures of shorter molecules with the simplified perturbed hard chain theory (SPHCT) equation of state. More recently, experiments and a theoretical (scaled Onsager) examination of binary mixtures involving rodlike liquid crystals of the same length but of different diameter have also shown that such systems can exhibit high-pressure (or high-concentration in the case of the experiments) regions of fluid immiscibility.[92–94] Our predictions indicate that for the aqueous solutions of PEG the lower-pressure and upper-pressure regions of liquid−liquid coexistence merge with the formation of an hourglass-shaped region of immiscibility for PEG molecular weights in excess of ∼73 900 g/mol. In the case of the water + PEG-2180 mixture the two-phase high-pressure region is not seen for the pressures examined, though it may still be present at pressures >4 GPa. As mentioned earlier, Sun and King[10] have reported a region of liquid−liquid immiscibility at high pressures of ∼0.5 GPa in a solution of water + PEG-21 000 that extends out to temperatures as low as 250 K; instead of the LLE region contracting with increasing pressure and disappearing altogether beyond a (hyper)critical point, the single-phase homogeneous mixture is bounded by a two-phase boundary that exhibits a turning point (maximum) at ∼0.55 GPa and 320 K. This type of behavior is also seen for water + PEG-270 000[9] and water + PEG-1 390 000.[10] The pressure dependence of the regions of liquid−liquid separation in aqueous mixtures is intricately linked to the structure of water in the solution (i.e., to the formation and disruption of hydrogen bonds). The unusual behavior found at high pressure for the aqueous solutions of PEG can be explained in terms of the disruption of water−PEG hydrogen bonding at elevated pressures.[9,11,95] One should point out, however, that this highly unusual trend could also be consistent with the appearance of three-phase (liquid−liquid−solid) coexistence involving ice states of water and not to boundaries of liquid−liquid miscibility, considering the high pressures (∼0.5 GPa), low temperatures (down to 250 K), and low concentrations of the PEG solutions that are involved; pure water freezes at 273 K, and the melting point of PEG ranges from 277−281 K for PEG-400 to 329−336 K for PEG-6000, but there will of course also be an appreciable depression of freezing point in the aqueous solutions. Though for aqueous solutions of higher molecular weight PEG a widening of the region of liquid−liquid immiscibility at high pressure is predicted with our SAFT approach, we do not reproduce the dramatic change in the slope of the critical locus of the LCSTs toward lower temperature found by Sun and King.[10] An initial increase in pressure in our SAFT calculations leads to more hydrogen bonding, so that a positive slope of the critical locus of the LCST with pressure is observed; in the case of low molecular weight PEG, the aqueous mixture becomes totally miscible above a hypercritical pressure. As the pressure is further increased, the unlike repulsive contributions become more dominant within our model and the homogeneous mixture becomes unstable above a certain threshold; a corresponding decrease in the extent of water−PEG hydrogen bonding is associated with this liquid−liquid immiscibility. For completeness we should also mention that, in addition to the regions of fluid phase coexistence discussed thus far, a separate region of liquid−liquid separation is predicted in our approach at very low temperatures (∼150 K) for all of the molecular weights of PEG considered. These low-temperature calculations should, however, be viewed with a certain degree of caution as the region is almost certainly

within the solid phase boundaries of the system, and any fluid would thus be metastable with respect to crystallization. This having been said, high-pressure phases of amorphous ice have been found at these low temperatures,[96,97] allowing for the possibility of an experimental window for the study of this metastable region of fluid-phase immiscibility.

4. Conclusions

The phase behavior of aqueous solutions of PEG has been studied using the SAFT-VR approach and a detailed model which takes into account water−water, PEG−PEG, and water−PEG hydrogen-bonding interactions as well as the size asymmetry between the solvent and the polymer. The transferable parameters describing the model molecules are determined by comparison with experimental data for the fluid phase equilibria of appropriate systems with a broad range of molecular weights. In the case of water we use a model that was developed in a previous study.[54] The parameters for the PEG molecules are determined from an examination of diethyl ether, which can be considered as the first member of the PEO polymer series, and from water + PEG liquid−liquid equilibrium data. Three unlike water−PEG interaction parameters (the binary water−PEG dispersive attraction, and the water−PEG(OH) and water−PEG(EO) hydrogen bonding) are also determined to ensure an optimal description of the liquid−liquid equilibrium of the mixtures. All of the parameters used within our approach are temperature independent and transferable to any molecular weight of PEG; the segment−segment parameters are independent of chain length, and the dependence on molecular weight is introduced via a linear relationship between the number of ethoxy groups in the polymer and the number of spherical segments m in the model chain. The firm molecular basis of the SAFT-VR approach allows for a good quantitative description of the characteristic water + PEG closed-loop regions of liquid−liquid immiscibility for all of the mixtures studied.

Our predictions of the water + PEG fluid phase behavior compare very favorably with those of other theoretical approaches. Karlström[27] reported only semiquantitative agreement using a conformational Flory−Huggins-based model for aqueous PEO-2290, -14 400, and -1 020 000. Using a similar model but with hydrogen bonding included explicitly, Matsuyama and Tanaka[29] obtained good agreement with the experimental data of Saeki et al.,[5] but the number of ethylene oxide segments n used to model the PEG polymers does not correspond consistently with the experimental molecular weight (e.g., $n = 10$ is used to describe PEG with a molecular weight of 2180 g/mol, when a value of $n \sim 50$ should have been used). In their pressure-dependent model, Bekiranov et al.[34] obtain fairly good agreement with the experimental data of Bae et al.[98] for molecular weights of 3350, 8000, and 15 000 g/mol by adjusting the intermolecular parameters to experimental LCST and UCST for a number of molecular weights; the resulting parameters are thus molecular weight dependent. Dormidontova[30] obtains a good description of the LLE for aqueous solutions of PEO of large molecular weight using a mean-field model taking into account water−water and water−PEO hydrogen bonding but does not discuss the change in pressure along the three-phase line. In a later paper,[31] the inclusion of hydroxyl end groups and PEO−PEO hydrogen bonding allows for a closer description of the experimental data over a larger range of molecular weights. There is, however, also an inconsistency in the number of ethylene oxide segments that is used in the model when compared to the experimental molecular weight. In the case of the methyl-terminated PEO model the lack of consistency between the experimental molecular weight and number of repeat units in the model for low molecular weights is attributed to polydispersity and the neglect of PEO−PEO hydrogen bonding. The inclusion of hydroxyl end groups (and PEO−PEO hydrogen bonding) leads to an improvement in the description, but inconsistencies still remain. Though there maybe a degree of uncertainty in the actual molecular weight of the polymer due to thermal degradation and polydispersity,[69] a linear relationship between the molecular weight and the number of repeat units should be expected for transferable segment parameters. An accurate prediction is possible when state-dependent parameters are used, as described by Tritopoulou et al.[17] (who report less than 15 K deviation for the LCSTs and UCSTs of a number of water + PEG mixtures), but at the expense of using temperature-dependent binary interactions which now play the role of an effective free energy.

In addition to the description of the closed loops of liquid−liquid immiscibility in the PEG systems, we have carried out a detailed analysis of the pressure dependence and complete $P-T-w$ surface. A clear advantage of using a continuum approach such as SAFT-VR is that the effect of pressure is incorporated in a natural way. Our theoretical calculations suggest that water + PEG mixtures exhibit type VI phase behavior in the classification of van Konynenburg and Scott.[84] For intermediate molecular weights of PEG the liquid−liquid separation is bounded by a hypercritical point with increasing pressure. Beyond this threshold pressure the mixture exists as a homogeneous liquid phase. A detailed understanding of the mechanism of this particular feature of the fluid phase separation in aqueous solutions of PEG could provide important generic insights into the link between hydrophobicity and denaturation of proteins.[86–90] At even higher pressures (∼GPa) a second region of liquid−liquid immiscibility which is bounded from below (in pressure) by a second hypercritical point is predicted for intermediate molecular weights of PEG. For large molecular weights the high pressure water + PEG phase behavior is predicted to exhibit an "hourglass" region of liquid−liquid immiscibility.

The development of a transferable approach based on the individual polymer segments is one of the particular strengths of our approach; this can be seen as an intermediate step toward a full group contribution treatment of the type described in recent work.[99] Our transferable models for the aqueous solutions of PEG provide us with a very convenient platform from which to investigate the competing roles of hydrogen bonding and size asymmetry in the appearance of LCSTs and closed-loop immiscibility as well as in the high-pressure re-entrant phase behavior, something we leave for a later study. As a final point, we note that for large molecular weight PEG one end of the polymer may be hydroxyl terminated and the other methyl terminated, depending on the particular polymerization process that is employed. The hydroxyl end can then be further methylated, leading to a degree of uncertainty as to the actual end-group termination of the PEG molecule. The specifics of the end-group termination can have an important bearing on the type of fluid-phase behavior that is observed in aqueous solution. An in-depth investigation of the effect of the PEG termination with our SAFT approach is also left for future work. Intramolecular (ring-like) association between the terminal OH groups on the same PEG chain may also be important for short to intermediate molecular weights; this type of association can also be treated within a Wertheim/SAFT approach.[100–102]

Acknowledgment. G.N.I.C. thanks ICI plc and the Engineering and Physical Sciences Research Council (EPSRC) of the UK for funding an Industrial Case studentship. Additional funding to the Molecular Systems Engineering group from the EPSRC (Grants

GR/N20317, GR/N03358, GR/N35991, GR/R09497, and EP/E016340), the Joint Research Equipment Initiative (JREI) (GR/M94427), and the Royal Society-Wolfson Foundation is also gratefully acknowledged.

References and Notes

(1) Zhu, H.; McShane, M. J. *Chem. Commun.* **2006**, 153–155.
(2) Malcolm, G. N.; Rowlinson, J. S. *Trans. Faraday Soc.* **1957**, *53*, 921–931.
(3) Hudson, C. S. *Z. Phys. Chem.* **1904**, *47*, 113–115.
(4) Jackson, G. *Mol. Phys.* **1991**, *72*, 1365–1385.
(5) Saeki, S.; Kuwahara, N.; Nakata, M.; Kaneko, M. *Polymer* **1976**, *17*, 685–688.
(6) Schneider, G. M. *Z. Phys. Chem.* **1963**, *37*, 333–352.
(7) Schneider, G. M. *Phys. Chem. Chem. Phys.* **2002**, *4*, 845–852.
(8) Garcia-Lisbona, M. N.; Galindo, A.; Jackson, G.; Burgess, A. N. *J. Am. Chem. Soc.* **1998**, *120*, 4191–4199.
(9) Cook, R. L.; King, H. E., Jr.; Peiffer, D. G. *Phys. Rev. Lett.* **1992**, *69*, 3072–3075.
(10) Sun, T.; King, H. E., Jr *Macromolecules* **1998**, *31*, 6383–6386.
(11) Briscoe, B.; Luckham, P. F.; Zhu, S. *J. Appl. Polym. Sci.* **1998**, *70*, 419–429.
(12) Hammouda, B.; Ho, D.; Kline, S. *Macromolecules* **2002**, *35*, 8578–8585.
(13) Paricaud, P.; Galindo, A.; Jackson, G. *Mol. Phys.* **2003**, *101*, 2575–2600.
(14) Patterson, D. *Macromolecules* **1969**, *2*, 672–677.
(15) Paricaud, P.; Galindo, A.; Jackson, G. *Ind. Eng. Chem. Res.* **2004**, *43*, 6871–6889.
(16) Garcia-Lisbona, M. N.; Galindo, A.; Jackson, G.; Burgess, A. N. *Mol. Phys.* **1998**, *93*, 57–71.
(17) Tritopoulou, E. A.; Pappa, G. D.; Voutsas, E. C.; Economou, I. G.; Tassios, D. P. *Ind. Eng. Chem. Res.* **2003**, *42*, 5399–5408.
(18) Smith, G. D.; Bedrov, D. *J. Phys. Chem. B* **2003**, *107*, 3095–3097.
(19) Clark, G. N. I.; Galindo, A.; Jackson, G. Submitted for publication.
(20) Ryu, D. Y.; Lee, D. H.; Jang, J.; Kim, J. K. *Macromolecules* **2004**, *37*, 5851–5855.
(21) Hirschfelder, J.; Stevenson, D.; Erying, H. *J. Chem. Phys.* **1937**, *5*, 896–912.
(22) Barker, J. A.; Fock, W. *Discuss. Faraday Soc.* **1953**, *15*, 188–195.
(23) Wheeler, J. C. *J. Chem. Phys.* **1975**, *62*, 433–439.
(24) Flory, P. J. *J. Chem. Phys.* **1941**, *9*, 660–661.
(25) Huggins, M. L. *J. Chem. Phys.* **1941**, *9*, 440.
(26) Staverman, A. J.; van Santen, J. H. *Recl. Trav. Chim. Pays-Bas* **1941**, *60*, 76.
(27) Karlström, G. *J. Phys. Chem.* **1985**, *89*, 4962–4964.
(28) Hu, Y.; Lambert, S. M.; Soane, D. S.; Prausnitz, J. M. *Macromolecules* **1991**, *24*, 4356–4363.
(29) Matsuyama, A.; Tanaka, F. *Phys. Rev. Lett.* **1990**, *65*, 341–344.
(30) Dormidontova, E. E. *Macromolecules* **2002**, *35*, 987–1001.
(31) Dormidontova, E. E. *Macromolecules* **2004**, *37*, 7747–7761.
(32) Sanchez, I. C.; Lacombe, R. H. *Macromolecules* **1978**, *11*, 1145–1156.
(33) Kleintjens, L. A.; Koningsveld, R. *Colloid Polym. Sci.* **1980**, *258*, 711–718.
(34) Bekiranov, S.; Bruinsma, R.; Pincus, P. *Phys. Rev. E* **1997**, *55*, 577–585.
(35) Poole, P. H.; Sciortino, F.; Grande, T.; Stanley, H. E.; Angell, A. A. *Phys. Rev. Lett.* **1994**, *73*, 1632–1635.
(36) Gil-Villegas, A.; Galindo, A.; Whitehead, P. J.; Mills, S. J.; Jackson, G.; Burgess, A. N. *J. Chem. Phys.* **1997**, *106*, 4168–4186.
(37) Galindo, A.; Davies, L. A.; Gil-Villegas, A.; Jackson, G. *Mol. Phys.* **1998**, *93*, 241–252.
(38) Blas, F. J.; Vega, L. F. *Mol. Phys.* **1997**, *92*, 135–150.
(39) Blas, F. J.; Vega, L. F. *Ind. Eng. Chem. Res.* **1998**, *37*, 660–674.
(40) Pedrosa, N.; Vega, L. F.; Coutinho, J. A. P.; Marrucho, I. M. *Ind. Eng. Chem. Res.* **2007**, *46*, 4678–4685.
(41) Pedrosa, N.; Pàmies, J. C.; Coutinho, J. A. P.; Marrucho, I. M.; Vega, L. F. *Ind. Eng. Chem. Res.* **2005**, *44*, 7027–7037.
(42) Hager, S. L.; Macrury, T. B. *J. Appl. Polym. Sci.* **1980**, *25*, 1559–1571.
(43) de Vringer, T.; Joosten, J. G. H.; Junginger, H. E. *Colloid Polym. Sci.* **1986**, *264*, 623–630.
(44) Maisano, G.; Majolino, D.; Migliardo, P.; Venuto, S.; Aliotta, F.; Magazú, S. *Mol. Phys.* **1993**, *78*, 421–435.
(45) Bieze, T. W. N.; Barnes, A. C.; Huige, C. J. M.; Enderby, J. E.; Leyte, J. C. *J. Phys. Chem.* **1994**, *98*, 6568–6576.
(46) Branca, C.; Magazú; S.; Maisano, G.; Migliardo, P.; Villari, V. *J. Phys.: Condens. Matter* **1998**, *10*, 10141–10157.
(47) Sasahara, K.; Sakurai, M.; Nitta, K. *Colloid Polym. Sci.* **1998**, *276*, 643–647.
(48) Magazú, S. *J. Mol. Struct.* **2000**, *523*, 47–59.
(49) Huang, L.; Nishinari, K. *J. Polym. Sci., Part B: Polym. Phys.* **2001**, *39*, 496–506.
(50) Tasaki, K. *J. Am. Chem. Soc.* **1996**, *118*, 8459–8469.
(51) Smith, G. D.; Bedrov, D.; Borodin, O. *Phys. Rev. Lett.* **2000**, *85*, 5583–5586.
(52) Kjellander, R.; Florin, E. *J. Chem. Soc., Faraday Trans. 1* **1981**, *77*, 2053–2077.
(53) Yu, M.; Nishiumi, H.; Arons, J. D. S. *Fluid Phase Equilib.* **1993**, *83*, 357–364.
(54) Clark, G. N.I.; Haslam, A. J.; Galindo, A.; Jackson, G. *Mol. Phys.* **2006**, *104*, 3561–3581.
(55) Jackson, G.; Chapman, W. G.; Gubbins, K. E. *Mol. Phys.* **1988**, *65*, 1–31.
(56) Jackson, G.; Gubbins, K. E. *Pure Appl. Chem.* **1989**, *61*, 1021–1026.
(57) Sako, T.; Wu, A. H.; Prausnitz, J. M. *J. Appl. Polym. Sci.* **1989**, *38*, 1839–1858.
(58) Kouskoumvekaki, I. A.; Krooshof, G. J. P.; Michelsen, M. L.; Kontogeorgis, G. M. *Ind. Eng. Chem. Res.* **2004**, *43*, 826–834.
(59) Spitzer, M.; Sabadini, E.; Loh, W. *J. Braz. Chem. Soc.* **2002**, *13*, 7–9.
(60) Green, D. G.; Jackson, G. *J. Chem. Soc., Faraday Trans.* **1992**, *88*, 1395–1409.
(61) Green, D. G.; Jackson, G. *J. Chem. Phys.* **1992**, *97*, 8672–8691.
(62) Galindo, A.; Whitehead, P. J.; Jackson, G.; Burgess, A. N. *J. Phys. Chem.* **1996**, *100*, 6781–6792.
(63) Jackson, G.; Rowlinson, J. S.; Leng, C. A. *J. Chem. Soc., Faraday Trans. 1* **1986**, *82*, 3461–3473.
(64) Press, W. H.; Teukolsky, S. A.; Vetterling, W. T.; Flannery, B. P. *Numerical Recipes in Fortran*, 2nd ed.; Cambridge University Press: New York, 1992.
(65) Fletcher, D. A.; McMeeking, R. F.; Parkin, D. *J. Chem. Inf. Comput. Sci.* **1996**, *36*, 746–749.
(66) Crupi, V.; Jannelli, M. P.; Magazú, S.; Maisano, G.; Majolino, D.; Migliardo, P.; Sirna, D. *Mol. Phys.* **1995**, *84*, 645–652.
(67) Frielinghaus, H.; Pedersen, W. B.; Larsen, P. S.; Almdal, K.; Mortensen, K. *Macromolecules* **2001**, *34*, 1096–1104.
(68) Hammouda, B.; Ho, D. L.; Kline, S. *Macromolecules* **2004**, *37*, 6932–6937.
(69) Bae, Y. C.; Lambert, S. M.; Soane, D. S.; Prausnitz, J. M. *Macromolecules* **1991**, *24*, 4403–4407.
(70) Haslam, A. J.; Galindo, A.; Jackson, G. *Fluid Phase Equilib.* **2008**, *266*, 105–128.
(71) Chapman, W. G.; Gubbins, K. E.; Jackson, G.; Radosz, M. *Fluid Phase Equilib.* **1989**, *52*, 31–38.
(72) Chapman, W. G.; Gubbins, K. E.; Jackson, G.; Radosz, M. *Ind. Eng. Chem. Res.* **1990**, *29*, 1709–1721.
(73) Barker, J. A.; Henderson, D. *J. Chem. Phys.* **1967**, *47*, 2856–2861.
(74) Barker, J. A.; Henderson, D. *J. Chem. Phys.* **1967**, *47*, 4714–4721.
(75) Boublík, T. *J. Chem. Phys.* **1970**, *53*, 471–472.
(76) Mansoori, G. A.; Carnahan, N. F.; Starling, K. E.; Leland, T. W. *J. Chem. Phys.* **1971**, *54*, 1523–1525.
(77) Barker, J. A.; Henderson, D. *Rev. Mod. Phys.* **1976**, *48*, 587–671.
(78) Chapman, W. G.; Jackson, G.; Gubbins, K. E. *Mol. Phys.* **1988**, *65*, 1057–1079.
(79) Kouskoumvekaki, I. A.; von Solms, N. IVC-SEP Ph.D. Summer School, **2002**.
(80) Borisova, I. A.; Erlykina, M. E.; Vatskova, V. G.; Sokolov, N. M.; Mikhailov, V. A. *Niitekhim* **1983**, *9*, 83.
(81) Bennett, G. M.; Philip, W. G. *J. Chem. Soc.* **1928**, *50*, 1930–1937.
(82) Kablukov, I. A.; Malischeva, V. T. *J. Chem. Soc.* **1925**, *47*, 1553–1561.
(83) Hill, A. E. *J. Chem. Soc.* **1923**, *45*, 1143–1155.
(84) van Konyenburg, P. H.; Scott, R. L. *Philos. Trans. R. Soc. London* **1980**, *298*, 495–540.
(85) Rowlinson, J. S.; Swinton, F. L. *Liquids and Liquid Mixtures*, 3rd ed.; Butterworth Scientific: London, 1982.
(86) Privalov, P. L.; Gill, S. J. *Adv. Protein Chem.* **1988**, *39*, 191–234.
(87) Privalov, P. L. *Crit. Rev. Biochem. Mol. Biol.* **1990**, *25*, 281–305.
(88) Ravindra, R.; Winter, R. *Chem. Phys. Chem.* **2003**, *4*, 359–365.
(89) Patel, B. A.; Debenedetti, P. G.; Stillinger, F. H.; Rossky, P. J. *Biophys. J.* **2007**, *93*, 4116–4127.
(90) Buldyrev, S. V.; Kumar, P.; Debenedetti, P. G.; Rossky, P. J.; Stanley, H. E. *Proc. Natl. Acad. Sci. U.S.A.* **2007**, *104*, 20177–20182.
(91) van Pelt, A.; Peters, C. J.; de Swaan Arons, J.; Deiters, U. K. *J. Chem. Phys.* **1995**, *102*, 3361–3374.
(92) Varga, S.; Galindo, A.; Jackson, G. *Mol. Phys.* **2003**, *101*, 817–825.
(93) Purdy, K. R.; Varga, S.; Galindo, A.; Jackson, G.; Fraden, S. *Phys. Rev. Lett.* **2005**, *94*, 057801.
(94) Varga, S.; Purdy, K. R.; Galindo, A.; Fraden, S.; Jackson, G. *Phys. Rev. E* **2005**, *72*, 051704.
(95) Briscoe, B.; Luckham, P.; Zhu, S. *Macromolecules* **1996**, *29*, 6208–6211.

(96) Finney, J. L.; Bowron, D. T.; Soper, A. K.; Loerting, T.; Mayer, E.; Hallbrucker, A. *Phys. Rev. Lett.* **2002**, *89*, 205503.
(97) Klug, D. D. *Nature (London)* **2002**, *420*, 749–751.
(98) Bae, Y. C.; Shim, J. J.; Soane, D. S.; Prausnitz, J. M. *J. Appl. Polym. Sci.* **1993**, *47*, 1193–1206.
(99) Lymperiadis, A.; Adjiman, C. S.; Galindo, A.; Jackson, G. *J. Chem. Phys.* **2007**, *127*, 234903.
(100) Sear, R. P.; Jackson, G. *Phys. Rev. E* **1994**, *50*, 386–394.
(101) Sear, R. P.; Jackson, G. *Mol. Phys.* **1996**, *87*, 517–521.
(102) Galindo, A.; Burton, S. J.; Jackson, G.; Visco, D. P.; Kofke, D. A. *Mol. Phys.* **2002**, *100*, 2241–2259.

MA8007898